Materials Advances

ROYAL SOCIETY OF CHEMISTRY

PAPER

View Article Online
View Journal | View Issue

Check for updates

Cite this: *Mater. Adv.*, 2021, 2, 4762

Efficient visible-light-driven hydrogen production by Zn–porphyrin based photocatalyst with engineered active donor–acceptor sites†

Nageshwarrao Chanda,[ab] Devulapally Koteshwar,[bc] Spandana Gonuguntla,[bd] Sreedhar Bojja,*[ab] Ujjwal Pal *[bd] and Lingamallu Giribabu *[bc]

Received 15th April 2021,
Accepted 7th June 2021

DOI: 10.1039/d1ma00342a

rsc.li/materials-advances

Here, we report a fine-tuned donor-π-acceptor concept based zinc-porphyrin-sensitized TiO_2 photocatalyst for the application in photochemical hydrogen evolution. The newly designed system showed unprecedented photocatalytic activity. The molecular structure comprises of 3-ethynyl phenothiazine as a donor moiety, porphyrin as a π-spacer, and either 3-(4-(benzo[*c*][1,2,5]thiadiazol-4-yl)phenyl)-2-cyanoacrylic acid (LG-22) or 3-(4-(benzo[*c*][1,2,5]thiadiazol-4-yl)thiophene-2-yl)-2- cyanoacrylic acid (LG-23) as an acceptor attached at *meso*-position of the zinc-porphyrin. Superior hydrogen generation efficiency has been keenly observed over PCT-LG-23 in correspondence with PCT-LG-22 and that of Pt–TiO_2 through visible light-induced photocatalytic water splitting. The effect of pH over photocatalytic hydrogen generation efficiency has been studied in the presence of triethanolamine (TEOA) which acts as a sacrificial electron donor (SED). LG-22 and LG-23 show H_2 production yields of 8850.9 μmol h^{-1} and 9793.5 μmol h^{-1} at pH = 12 and pH = 3, respectively with a high turnover number (TON was 11801.2, 13058 for LG-22 and LG-23, respectively) under light irradiation with apparent quantum yields (AQY) of 7.20% and 7.96% for LG-22 and LG-23, respectively. The presence of thiophene and Benzo[1,2-*b*:4,5-*b*′]dithiophene (BDT) facilitated the extended π-conjugation, which gave rise to the excited state electronic properties and basicity of thiophene that enhanced the light absorption capacity of LG-23 in acidic conditions. Thus, this work provides a prime example of more efficient photonic conversion of an already existing, moderately active Zn porphyrin synthetic complex core encompassed precisely positioned functionalities of thiazine.

1. Introduction

The development of efficient and stable photocatalysts for water splitting tends to be a key challenge over the energy conversion domain.[1] Recently, several groups of scientists have been focusing on engineering different functionalities in dyes for solar to chemical fuel conversion. The dye sensitization is a viable approach for the generation of clean fuel through water splitting by means of solar to chemical energy conversion process.[2] This biomimetic blueprint has been explored intensively over the last two decades. The design and construction of new sensitizers can emulate natural photosynthesis to maximize photon conversion.[3] Due to the wider band gap and low ability to undergo photogenerated charge carrier separation, the efficacy of TiO_2 semiconductors could be enhanced significantly by sensitizing with light absorber dye or photosensitizers, which tends to be the key component in engineering the dye-sensitized photocatalyst meticulously.[4] Several technologies such as metal complexes,[5] metal-free organic photosensitizers,[6] and inorganic dyes,[7] have been used till now in hydrogen production. Among various feasible strategies, porphyrin-based donor-π-acceptor (D-π-A) dyes provide high flexibility for the development of efficient light-harvesting system.[8]

They tend to possess a similar structure resembling the structure of chlorophyll and appear to be a promising energy harvesting system in the domain of artificial photosynthesis.[9] The synthetic analogues of porphyrin sensitizers show a strong intense Soret band (~420 nm) and less intense Q-band (500–750 nm) in its optical absorption spectra and easily tunable energy levels to maximize photon conversion.[10] Earlier research on porphyrin-based systems was predominantly focused on the limited chromophoric groups and π

[a] *Department of Analytical and Structural Chemistry, CSIR-Indian Institute of Chemical Technology, Hyderabad-500007, India. E-mail: sreedharb@iict.res.in*
[b] *Academy of Scientific and Innovative Research (AcSIR), Ghaziabad, UP, India. E-mail: upal03@gmail.com*
[c] *Polymers and Functional Materials, CSIR-Indian Institute of Chemical Technology, Hyderabad-500007, India. E-mail: giribabu@iict.res.in*
[d] *Department of Energy and Environmental Engineering, CSIR-Indian Institute of Chemical Technology, Hyderabad-500007, India*

† Electronic supplementary information (ESI) available. See DOI: 10.1039/d1ma00342a

conjugation. Moreover, of all these classes of sensitizers, the porphyrin-based sensitizers act as light harvesters on semiconducting materials for an efficient conversion of solar energy to clean chemical hydrogen energy, and their operating mechanism closely follow the path of DSSC.[11] In this direction, most of earlier works determine the modification of anchoring groups either at the β-pyrrole position or at *meso*-phenyl position of the porphyrin macrocycle.[12] While looking at the D-π-A concept, tuning their donor and acceptor moieties broadly increases the device performance up to many folds. Until now, remarkable energy conversion efficiencies have been achieved through the usage of ruthenium polypyridyl complex and zinc porphyrin dyes as photosensitizers by the devices of DSSC.[13] Various zinc porphyrin dyes with D-π-A architecture have been reported so far. Due to the large planar π-conjugated structure of porphyrins, they tend to possess intrinsic characteristics including photon absorption, high thermal stability, efficient electron transfer, absorption in UV-near IR region, high fluorescence, and efficient light harvesting properties, which tend to act as light harvesters on semiconducting materials suitable for both DSSC and visible light-induced hydrogen generation activity.[14] According to Liao *et al.*, PdTAPP-TFPT resulted in superior photocatalytic activity of 30 880 μmol g^{-1} whereas 1970 μmol g^{-1} using Pt@PdTAPP-TFPT under aqueous sodium ascorbate solution with the light irradiation of 420 nm intensity.[15] Chen *et al.*, reported the superior hydrogen generation activity of 43 μmol h^{-1} using ZnCoDETPP photocatalyst and triethanolamine (TEOA) under the irradiation of Xe lamp (300 W) equipped with $\lambda \geq 400$ nm cut off filter.[16] Li *et al.*, reported 2% ZnTCPP/g-C_3N_4 (900 μmol g^{-1} h^{-1}) and 2% ZnTPP/g-C_3N_4 (681 μmol g^{-1} h^{-1}) in aqueous triethanolamine (TEOA) under 300 W Xenon arc lamp.[17] Huang *et al.*, reported that Pt/THPP-Pd-TiO_2 resulted in the superior activity of 2025.4 μmol g^{-1} h^{-1} as compared to Pt/THPP-Zn-TiO_2, which has superior activity of 1239.8 μmol g^{-1} h^{-1}, respectively, under the similar conditions of TEOA having $\lambda > 420$ nm.[18] Guo *et al.*, reported that TiO_2 MS-Cu-TCPP resulted in an enhanced hydrogen production activity of 1.35 mmol g^{-1} h^{-1} in TEOA aqueous solution.[19] Zhang *et al.*, reported that SA-TCPP composite tends to possess hydrogen generation activity of 40.8 μmol g^{-1} h^{-1} in aqueous TEOA solution under the irradiation of 300 W Xenon lamp.[20] Xi *et al.*, reported that 10% ZnO NR-Cu-TSPP tends to possess 3.25 mmol g^{-1} hydrogen generation activity under the irradiation of 300 W Xenon lamp in aqueous triethanolamine (TEOA) solution.[21] Tritton *et al.*, depicted that TBPyZnP-Ir displayed high photocatalytic hydrogen generation activity of 16.12 mmol g^{-1} h^{-1} within 5 h of irradiation in triethylamine (TEA).[22]

The success in designing new sensitizers and the molecular engineering of photosensitizers culminated over the periods in our group and, in particular, the porphyrin-based sensitizers with D-π-A concept-based porphyrin sensitizers such as LG-5, LG-DtT, and LG-tT series of sensitizers include the replacement of 4-ethynyl thiophene in the LG-5 moieties by thieno thiophene (LG-tT) or dithieno thiophene (LG-DtT) majorly acting as auxiliary acceptor and cyanoacrylic acid as the anchoring group over the synthesized materials.[23–25] The power conversion of the PHPT-LG5, PCT-LG-DtT, PCT-LG-tT materials over the Pt-HPT/cTiO$_2$ moiety was recorded as 10.20%, 8.25%, and 7.05%, respectively, with the photocatalytic hydrogen generation efficiencies of 2691, 6641, and 7396 μmol g^{-1} h^{-1}, respectively.

In continuation of our efforts towards the development of efficient photocatalysts, we replace the acceptor groups in LG-5, LG-DtT, and LG-tT series of sensitizers with either 3-(4-(benzo[c][1,2,5]thiadiazol-4-yl)phenyl)-2-cyanoacrylic acid (LG-22) or 3-(4-(benzo[*c*][1,2,5]thiadiazol-4-yl)thiophene-2-yl)-2-cyanoacrylic acid (LG-23) as an acceptor attached at *meso*-position of the zinc-porphyrin. The hydrogen generation results envisage that PCT-LG-23 tends to possess superior hydrogen generation efficiency of 9793.5 μmol g^{-1} h^{-1} under acidic conditions (pH-3) in comparison with that of PCT-LG-22 and Pt/TiO_2. The role of variation of pH and SED which merely occurs due to the basicity and interaction of moieties with the acidic moieties has been clearly explained. This study paves a crucial way for the zinc porphyrin-based sensitizers in the field of hydrogen generation and energy conversion. The structures of zinc porphyrin dyes are shown in Scheme 1. In this regard, our continuous efforts to develop two new simples and efficient zinc porphyrin ring dyes, stable and cost-effective sensitizer dyes involving fewer synthetic steps of trans A_2BC porphyrin Zn(II) complexes LG-22 and LG-23 were successful.

2. Experimental

All the reagents were commercially available. The commercial TiO_2 (cTiO$_2$), chloroplatinic acid (H_2PtCl_6) (8 wt% solution),

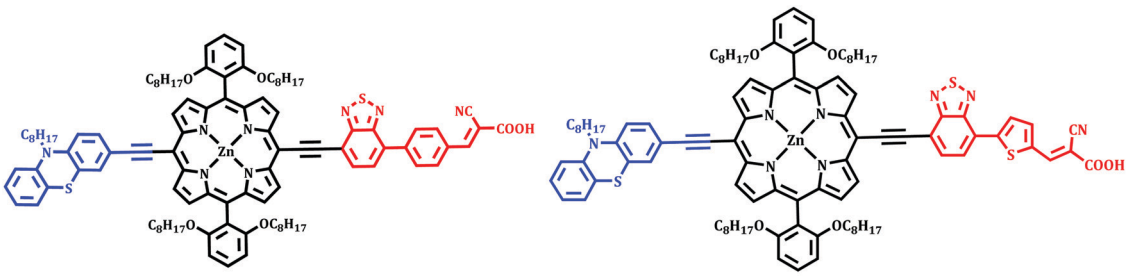

LG22: 3-(4-(benzo[c][1,2,5]thiadiazol-4-yl)phenyl)-2-cyanoacrylic acid LG-23: 3-(4-(benzo[c][1,2,5]thiadiazol-4-yl)thiophene-2-yl)-2-cyanoacrylic acid

Scheme 1 Dye structures of LG22 and LG23.

triethanolamine (TEOA) were purchased from Sigma-Aldrich, USA. The procured chemicals are of reagent grade and are highly pure for synthesis. Both porphyrin sensitizers were synthesized as per methods reported in the literature.[26]

2.1. Preparation of platinized titanium dioxide (Pt–TiO_2)

To enhance the photocatalytic H_2 generation efficiency, 1 wt% of Pt metal was deposited over the TiO_2 semiconducting material surface as reported previously.[27] The preparation follows a certain criteria involving the dispersion of 0.1 g of TiO_2 in 30 mL of methanol followed by the addition of 0.25 mL (8 wt%) of H_2PtCl_6 over the above-mentioned suspension. It was then subjected to the light radiation of 300 W Xenon lamp resulting in the color change of the composite into grey color which was collected through centrifugation and washed using water and ethanol and was subjected to drying at 70 °C in the vacuum oven. The resultant product so obtained was named as Pt/TiO_2.

2.2. Preparation of dye adsorbed Pt/TiO_2 photocatalyst

The typical synthesis procedure follows a previously reported standard method.[27] 0.5 μmol of the dye was subjected to ultrasonication in a 100 mL round bottom flask (RBF) containing a solution mixture of ethanol and acetonitrile in 1 : 1 vol% with a total volume of 20 mL. Further addition of 100 mg of Pt/TiO_2 was carried out in the RBF, which was stirred under dark conditions over a period of 24 h and wrapped using aluminum foil in order to avoid unwanted photochemical reactions. The final products were collected through centrifugation and filtration using water and ethanol and were subjected to drying under vacuum at 50–60 °C and the final composites were named as PCT-LG-22 and PCT-LG-23.

2.3. Photocatalytic hydrogen generation experiments

Photocatalytic hydrogen gas generation procedure has been carried out in a 100 mL Pyrex glass-based photoreactor equipped with an external cooling system, loaded with 20 mL aqueous solution of triethanolamine (TEOA), and suspended with 10 mg of the photocatalyst. The pH of the solution is maintained using conc. HCl solution. The role of TEOA is that it acts as a sacrificial electron donor (SED). The whole system was sealed using a rubber septum in order to make it air tight and an inert atmosphere has been created using evacuation and nitrogen purging procedure. The system was placed 25 cm away from the light source and the light irradiation was carried out using 300 W Xenon arc lamp (Newport, USA). The gas analysis process was carried out after every 1 h using a Gas Chromatograph (PerkinElmer Claurus 590 containing molecular sieve/5 Å column, USA) equipped with TCD and N_2 flow. Turnover number (TON) is the number of reactive dye molecules with the semiconducting material to that of the active sites. The calculation is displayed in ESI.†

Photoelectrochemical measurements. All the photoelectrochemical measurements have been carried out in a three-electrode system using a potentiostat (CH instruments, CHI 6005E, USA) with 0.5 M Na_2SO_4 (pH ≈ 6.5) aqueous electrolytic solution using Ag/AgCl saturated with KCl as reference electrode, Pt wire as counter electrode, and sample loaded modified ITO film as a working electrode. The sample loading over the ITO film with a surface area of 2 × 2 cm^2 has been carried out by the dispersion of 5 mg of the sample into 500 μmol ethanol and 20 μmol of Nafion through ultrasonication and drop casted over the ITO film and dried at 50 °C. The irradiation of the electrodes has been carried out using a 300 W Xe lamp equipped with an AM 1.5 G, 100 mW cm^{-2} light intensity. EIS of the composites has been keenly recorded with an applied open-circuit voltage and potential frequency range of 1 MHz to 1 Hz with an AC amplitude of 10 mV.

Characterization studies. Various characterization techniques such as powder X-ray diffraction (XRD), scanning electron microscopy (SEM), and transmission electron microscopy (TEM) have been highly useful for phase and structural determination. Diffuse reflectance spectroscopy (DRS), fluorescence and time-dependent photoluminescence spectroscopy have been carried out for optical properties. Photoelectrochemical properties were studied by CH instruments such as CV, Photocurrent measurements, and Nyquist Plot. The functional group analysis was performed by FT-IR spectroscopy. The photocatalytic hydrogen generation experiments were carried out using 300 W Xenon arc lamp (Newport, USA). The gas chromatography analysis was performed by a gas chromatograph (PerkinElmer Claurus 590, USA) equipped with a TCD detector under an inert atmosphere of nitrogen functioning as carrier gas.

3. Results and discussion

Both the sensitizers were synthesized as per literature methods and characterized by ^{1}H NMR and MALDI-MS spectroscopies (Fig. S1 to S4, ESI†).[26] The presence of molecular ion peak in both the sensitizers confirms the molecular integrity of the sensitizers. Further, molecular integrity of both the sensitizers were further supported by ^{1}H NMR spectra studies (Fig. S1 to S4, ESI†).

3.1. Morphological studies

The phase structure and crystallinity of the prepared catalysts were observed by XRD studies. As shown, the resultant peaks were obtained at 25.55°, 38.10°, 48.24°, 54.19°, 55.24°, and 62.96° which indicates the (101), (103), (200), (105), (211), and (204) planes, respectively, in comparison with the standard JCPDS 21-1272 file of anatase TiO_2 (Fig. 1a).[28] It clearly envisages that the 2θ values of cTiO_2, Pt/TiO_2, calcined Pt/TiO_2 are similar in correspondence with the crystalline commercial phase of cTiO_2 according to the JCSPDS file respectively. The main peak at ~25 °C of all (cTiO_2, Pt/TiO_2, calcined Pt/TiO_2) samples was very sharp indicating the crystalline nature of the samples. The scanning electron microscopy studies shown in Fig. 1b–e depict the mesoporous particle nature of pristine TiO_2 and no specific morphological changes have been identified in the as-prepared Pt/TiO_2, PCT-LG-22, and PCT-LG-23. The mesoporous

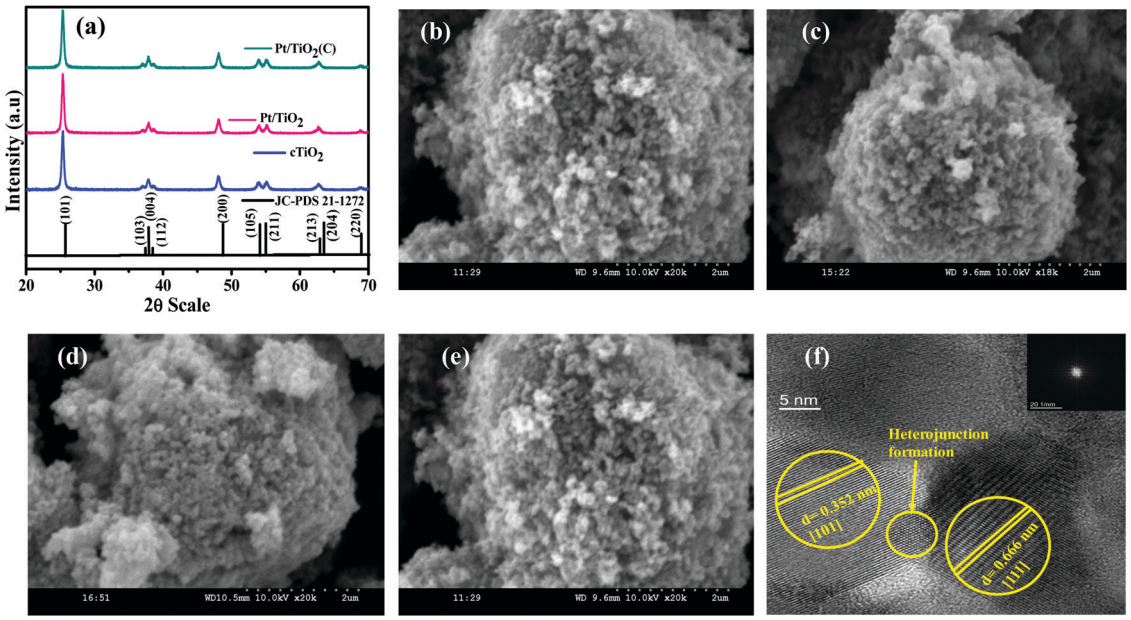

Fig. 1 (a) XRD Pattern of $cTiO_2$, Pt/TiO_2, Pt/TiO_2 (calcined) and JCPDS file, SEM analysis of (b) $cTiO_2$, (c) Pt/TiO_2, (d) PCT-LG-22, and (e) PCT-LG-23, (f) TEM analysis of the Pt/TiO_2.

morphology of the compounds increases the electron–hole diffusion kinetics.

The morphological phases of $cTiO_2$ over the Pt/TiO_2 photocatalyst were further confirmed by TEM analysis. The lattice spacing of 0.357 nm relates to the (101) plane of the Commercial phase of TiO_2 and that of the noble metal loading *i.e.*, Pt tends to be in the (111) phase with 0.66 nm as shown in Fig. 1f. The formation of the heterojunction among TiO_2 and Pt has been clearly visualized, which is highly favorable to enhance the hydrogen generation and thereby absorb dye over the surface.

3.2. Optical properties

The absorption studies of the $cTiO_2$, Pt/TiO_2, dye moieties, and the dye-loaded final composites were carried out in order to understand the light harvesting nature of the materials. The results present in Fig. S5a (ESI†) clearly envisage that LG-22 and LG-23 tend to possess higher absorption of light due to the intense porphyrin moieties. The THF processed LG-22 display intense peaks of Soret band in the region of ~448 nm ($\log \varepsilon$ = 4.62 M^{-1} cm^{-1}) and 679 nm ($\log \varepsilon$ = 4.18 M^{-1} cm^{-1}) due to π–π* transition whereas LG-23 reveals the peaks at ~452 nm ($\log \varepsilon$ = 4.40 M^{-1} cm^{-1}) and 701 nm ($\log \varepsilon$ = 4.30 M^{-1} cm^{-1}), which are majorly present due to the extended π-conjugation of the thiophene moieties (Fig. S5, ESI†).[25] Further, the onset of LG-22 sensitizer extends up to 800 nm whereas in the case of LG-22 it extends up to 750 nm only (Fig. S5a, ESI†). These results envisage that LG-23 plays a vital role in order to enhance the conjugation and change the ground state of LG-23 compared to that of LG-5 and LG-22. The change in the peak intensities and their corresponding light absorption has been clearly visualized in Fig. S5c (ESI†). When compared with that of Fig. S5b and d (ESI†), it can be clearly observed that the light absorption capacities of PCT-LG-22 and PCT-LG-23 are superior compared to that of $cTiO_2$ and Pt/TiO_2, whereas it can also be observed that the peak intensity decreases in comparison with that of the dye moieties indicating the absorption of the dye moieties over Pt/TiO_2. The Tauc Plots shown in Fig. 2a and Fig. S5d (ESI†) envisage that the initial band gap of $cTiO_2$ is 3.2 eV which has been gradually decreased by the deposition of Pt over the surface of TiO_2 to 3.0 eV whereas that of PCT-LG-22 and PCT-LG-23 are 2.93 eV and 2.89 eV, respectively.[29] The emission spectra shown in Fig. S5e (ESI†) suggest that the quenching and red shift has been significantly observed in the LG-23 moiety at 752 nm, which is due to the strong interactions between the dye and the semiconducting material and thiophene rings in LG-23. The peak intensity of LG-22 is found to be at a wavelength range of 675–750 nm with broad peak π–π* interactions.

Fourier transform infrared (FT-IR) spectroscopy. Fourier transform infrared spectroscopy is an important technique to determine the presence of different functional groups over a molecule. The peaks at 3400–3500 cm^{-1} depicts the presence of O–H acid function group, the peak at 2600–2800 cm^{-1} shows the presence of C═C–H hydrogen group, and that at 2200–2300 cm^{-1} indicates the presence of a C≡N group (Fig. S2, ESI†).[23] Furthermore, it is known that the peak appearing in the 1500–1600 cm^{-1} region indicates the existence of the C═C aromatic ring group. The peak at 1690–1700 cm^{-1} indicates the presence of C═O group in LG-22, LG-23 compounds and strong interactions and binding between the dye and the TiO_2 moieties have been clearly indicating the superior light absorption capacities.

Fig. 2b demonstrates the emission spectra of both the catalysts through the photoluminescence studies. The results envisage that there is a blue shift in the emission intensities of PCT-LG-22, PCT-LG-23 in comparison with that of LG-22, LG-

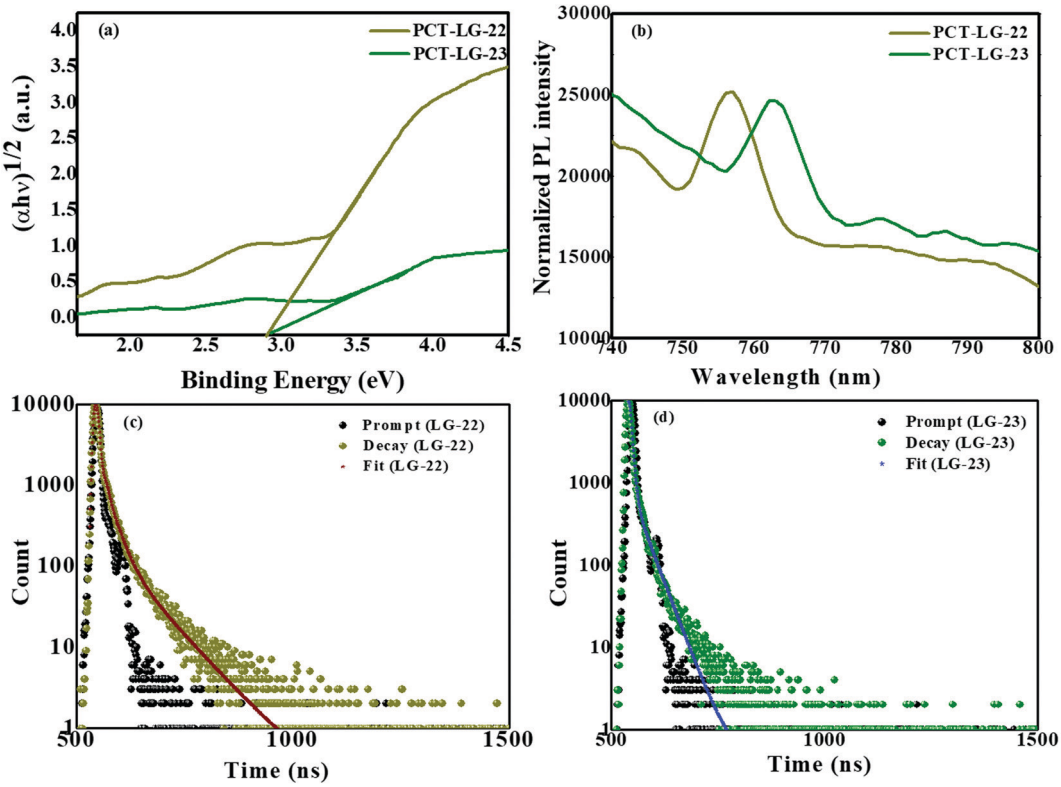

Fig. 2 (a) Tauc Plot of PCT-LG-22, PCT-LG-23, (b) Photoluminescence spectra of PCT-LG-22, PCT-LG-23, TCSPC plot of (c) PCT-LG-22, and (d) PCT-LG-23.

23. The decrease in the luminescence emission intensity of the composites in comparison with LG-22, LG-23 is due to the efficient electron-charge transfer among Pt/TiO_2 and the dye molecules and faster electron-charge transfer. The single excited-state lifetime of both the dye-loaded PCT samples resulted in the nanometric range of the bi-exponential transformation as shown in Fig. 2c and d, and their respective average lifetimes have been tabulated in Table 1. The average lifetime of PCT-LG-22 is 0.3 ns whereas that of PCT-LG-23 is 0.5 ns as shown in Table 1. The result trend indicates the faster relaxation time of photoexcited charges, which indicates directly the photocatalytic efficiency confirming the electron–hole recombination kinetics.

Theoretical study. In order to further clearly visualize the structural and electronic properties of the proposed dyes LG-22 and LG-23, computational studies by adopting density functional theory (DFT) and TDFT studies at B3LYP/6-31G (d,p) level using the Gaussian 09 program have been carried out as shown in Table 1 and 2.[30,31] The figures shown in Table 2 visualize the butterfly structures of the phenothiazine moieties connected at the *meso*-position of the porphyrin core with non-planarity. Long octyloxy chains over the *meso*-phenyl position lead to a decline in the electron–hole charge recombination kinetics over the conduction band of TiO_2. The DFT studies of LG-22 and LG-23 reveal that the HOMO is present mostly over the phenothiazine donor part and porphyrin bridge whereas the LUMO values are located over the BDT auxiliary acceptor for both the sensitizers. The transition between the HOMO to LUMO in the porphyrin sensitizers promotes intermolecular charge-transfer capacity over the excitation of electrons and charge separation states. The HOMO–LUMO values shown in Table 3 of LG-22 and LG-23 are 1.745 eV and 1.603 eV, respectively, determining the superior light absorption capacity and the conduction valence band values have been calculated through CV studies.

Table 1 Lifetime measurements of the composites

Catalyst (dye)	τ_1 (ns)	τ_2 (ns)	τ_3 (ns)	Average emission lifetime (Ave. τ) (ns)
PCT-LG-22	0.24	0.89	—	0.3
PCT-LG-23	0.56	0.11	0.22	0.5

Photocatalytic hydrogen generation. In order to elucidate the efficiencies of these proposed dyes in photocatalytic hydrogen generation reactions, the photocatalytic hydrogen production analysis of dye-loaded Pt/TiO_2 has been investigated over an aqueous TEOA solution (20 vol%) by the addition of conc. HCl in order to maintain the pH of the required solution. Furthermore, in order to optimize the effect of pH over the hydrogen generation activity, we have carried out a series of experiments with pH variation under similar conditions and the results have been incorporated in Fig. 3. It is evident that PCT-LG-23 at pH-3 resulted in superior activity compared to PCT-LG-22 at 9,793.5 μmol g^{-1} h^{-1} whereas PCT-LG-22 tends to possess higher hydrogen generation efficiency at pH-12 as 8,850.9 μmol g^{-1} h^{-1}, respectively (Fig. 3a and Fig. S3, ESI†), the thiophene moieties over LG-23 due to high basicity tends to react with HCl at lower temperatures whereas LG-22 possess a

Table 2 Optimized energies, HOMO–LUMO energies using DFT studies carried out using B3LYP/6-31G (d,p) in vacuum

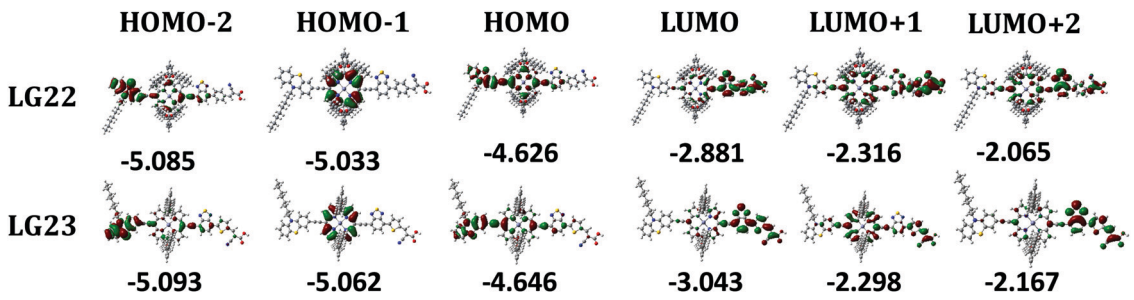

Table 3 Physico-chemical properties of the dye

Dye	E,[a] kcal mol^{-1}	λ_{max} (absorption) (nm)	λ_{max} (emission) (nm)	HOMO (H)[b]	LUMO (L)[b]	H–L gap[b]	μ[c]
LG22	−4 704 209	650	710	−4.626	−2.881	1.745	12.8893
LG23	−4 905 491	720	755	−4.646	−3.043	1.603	12.0219

[a] Total energy of LG22 and LG23. [b] Values in eV. [c] Values in Debye units.

benzene ring with delocalization of pi electrons and possess lower hydrogen generation efficiency.[32] The results when compared to our previous work of LG-5 reveal that PHPT-LG5 resulted in 4196 μmol g^{-1} h^{-1} at pH-7. The contradictory results might be due to the change in the acceptor moieties. The presence of thiophene auxiliary moieties over the PCT-LG-23 facilitates higher absorption of the electrons in the acidic solution making it more reactive and enhances the electron–hole recombination kinetics, which clearly increases the light absorption and water splitting with superior hydrogen generation activity which tends to be in correlation with the reported photosensitizers as tabulated in Table S1 (ESI). The recyclability studies shown in Fig. 3b indicate that the molecules are highly stable up to 5 cycles and their efficiency has been maintained constantly throughout the reaction.

4. Photo electrochemical studies (PEC)

The photoelectrochemical studies can be thoroughly examined in order to determine the charge-transfer kinetics over the as-synthesized moieties. The photoelectrochemical studies such as EIS, CV, Nyquist Plot, time dependency of the photocurrent profiles, and the Mott–Schottky plots have been analyzed and are shown in Fig. 4.

The EIS of the composites was performed at a specified voltage of −0.9 V *vs.* NHE in order to determine the change in the current under dark and light conditions which can be visualized in Fig. 4a. The profiles reveal that PCT-LG-23 tends to possess superior electron transfer reaction kinetics with higher reactivity of the chemically active species. The Nyquist plot of Pt/TiO_2, PCT-LG-22, and PCT-LG-23 consisting of TiO_2 in contact with the platinum and the loaded interfaces of dye moieties are shown in Fig. 4b. The smaller arc radius of PCT-LG-23 reveals higher charge separation efficiency which explains the electron charge recombination kinetics. The charge recombination kinetics of these materials can be seen as a semicircle with an ohmic resistance of 84.4 Ω, 41.8 Ω, and 55.7 Ω for Pt/TiO_2, PCT-LG-22 and PCT-LG-23 respectively, indicating a greater electron–hole recombination resistance of PCT-LG-23 thereby decreasing the charge recombination

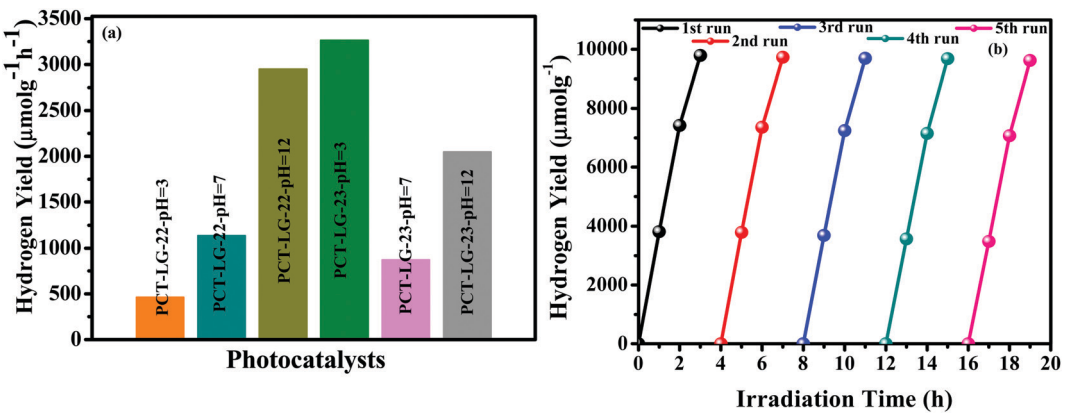

Fig. 3 (a) Histogram determining different pH variations of PCT-LG-22 and PCT-LG-23, and (b) Recyclability measurements of the synthesized composites.

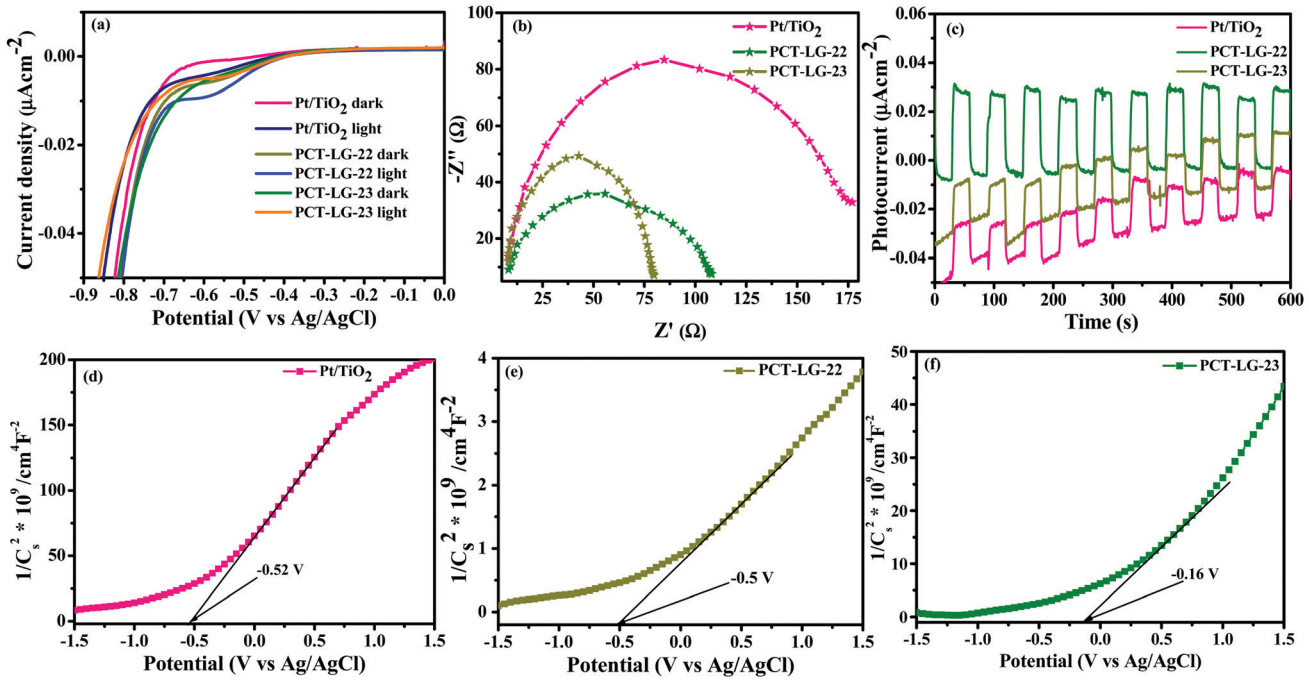

Fig. 4 (a) EIS, (b) Nyquist plot, (c) transient photocurrent measurements of Pt/TiO_2, PCT-LG-22 and PCT-LG-23 respectively, Mott–Schottky plots of (d) Pt/TiO_2, (e) PCT-LG-22, and (f) PCT-LG-23.

dynamics. Fig. 4c shows the time-dependent photocurrent profiles of as-synthesized PCT-LG-22, PCT-LG-23 ad Pt/TiO_2 upon cyclic on/off irradiation of light with an intensity of 100 mW cm^{-2}, $\lambda > 420$ nm. The initial photocurrent measurement of PCT-LG-23 is 34.4 mA cm^{-2}, which is comparatively superior to that of PCT-LG-22 and Pt/TiO_2 determines the gradual decrease of intensity with the light off and increase of intensity with the light on determining the stability of the catalyst for a larger lifetime with their stable photocurrent values consistent with the EIS and Nyquist data. The Mott–Schottky data of the samples shown in Fig. 4d–f reveals the flat band potentials as 2.68 eV, 2.7 eV, and 3.04 eV with the values of −0.52 V, −0.5 V, 0.16 V for Pt/TiO_2, PCT-LG-22, PCT-LG-23, respectively, which closely interrelates to the band gap kinetics of the composites.

The redox properties are very essential in order to estimate the HOMO–LUMO levels of both the sensitizers. For this reason, we have performed the CV of both sensitizers in THF solvent using 0.1 M tetra butyl ammonium hexafluorophosphate ($TBAPF_6$) as the supporting electrolyte. Each sensitizer undergoes a reversible oxidation peak at ∼0.92 V *vs.* Ag/AgCl and a quasi-reversible reduction at ∼−1.40 V *vs.* Ag/AgCl. The energy level diagram of the mechanistic interface of the LG-22 and LG-23 dyes in comparison with that of the LG-5 dye has been shown in Fig. 5a, which indicated the dye regeneration tendency and electron-injection over Pt/TiO_2 from the dye molecules. The CV studies of both the LG-22 and LG-23 dyes along with the dye-loaded Pt/TiO_2 samples have been analyzed to depict the redox potentials and their consecutive properties. The same has been observed in the

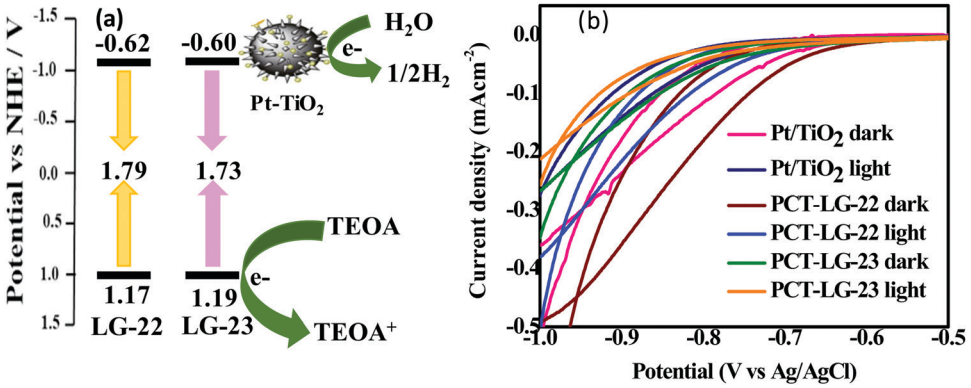

Fig. 5 (a) Mechanism of electron transfer kinetics, and (b) cyclic voltammetry of PCT-LG-22, PCT-LG-23.

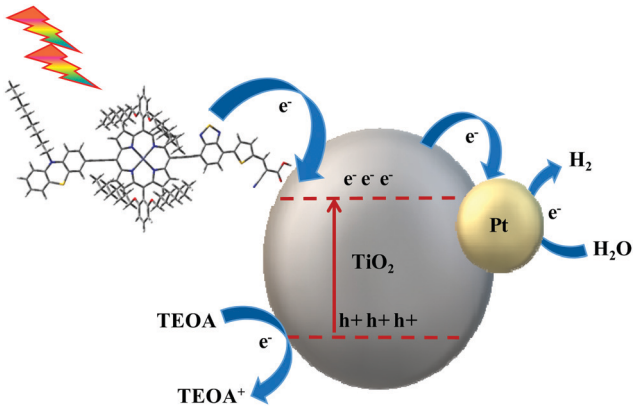

Fig. 6 Schematic representation of photocatalytic hydrogen production.

dark and light conditions of the dye-loaded Pt/TiO_2 moieties in Fig. 5b.

The dyes investigated in the photocatalytic system played an important role on the TiO_2 surface. It improves light harvesting as well as leads to effective electron injection to the surface of the catalyst as shown in Fig. 6. In this study, the fast charge transfer from the dye to the semiconductor minimizes the charge recombination reactions and increases efficiency. This observation clearly suggests that the hydrogen generation path is controlled by the following major steps: upon photoirradiation, (i) the electron injection from the excited state of the dye molecules into the conduction band of TiO_2 under controlled charge transfer process, (ii) charge recombination dynamics among the injected electron and the sensitizer radical cation, (iii) reduction of dye radical cations through TEOA, (iv) collection of electrons injected at Pt sites to result in hydrogen evolution. The cocatalyst Pt provides active sites at the TiO_2 surface for catalytic reactions.

Mechanistic pathway$Pt/TiO_2/LG22$ **or** $LG23 + h\nu \rightarrow Pt/TiO_2/LG22^*$ **or** $LG23^*$

$$Pt/TiO_2/LG22^* \text{ or } LG23^* \rightarrow Pt/TiO_2(e^-)/LG22^{\bullet+} \text{ or } LG23^{\bullet+} \quad \text{(i)}$$

$$Pt/TiO_2/LG22^* \text{ or } LG23^* \rightarrow Pt/TiO_2/LG22 \text{ or } LG23 + \text{heat} + h\nu_F \quad \text{(ii)}$$

$$Pt/TiO_2(e^-)/LG22^{\bullet+} \text{ or } LG23^{\bullet+} + TEOA \rightarrow Pt/TiO_2(e^-)/LG22 \text{ or } LG23 \quad \text{(iii)}$$

$$Pt/TiO_2(e^-)/LG22 \text{ or } LG23 + H^+ \rightarrow Pt/TiO_2(e^-)/LG22 \text{ or } LG23 + 1/2H_2 \quad \text{(iv)}$$

A sensitizer is one of the vital components in succeeding high efficiency and durability of the DSSC device. A dye-sensitized solar cell is a photoelectrochemical device that contains a photoelectrode, a I^-/I_3^- redox coupled electrolyte, and a counter electrode. The crucial factor of the sensitizer is light harvesting in the visible region. Here, LG-22 and LG-23 act as photo sensitizers as they are capable of absorption in the visible region 400–800 nm. The sensitizer absorbs light at three different wavelengths *i.e.*, 350–400 nm, 440–450 nm, and 700–720 nm, which covers the whole visible region and even a part of the near-IR region. When loaded with Pt–TiO_2, the sensitizer avoids the multi-layer adsorption on the semiconductor surface as the sensitizer hasan anchoring group cyanoacetic acid, which strongly binds the dye onto the semiconductor surface.

5. Conclusion

The panchromatic LG-22 and LG-23 dyes were designed and synthesized with fine-tuning of the acceptor moieties in LG-22 and LG-23 loaded over Pt/TiO_2 for the application in photocatalytic hydrogen generation. The PCT-LG-23 composite resulted in the superior activity of 9793.5 μmol g^{-1} h^{-1} at pH-3, whereas PCT-LG-22 showed the hydrogen evolution efficiency of 8850.9 μmol g^{-1} h^{-1} from the aqueous mixture of TEOA. The intermolecular hydrogen interactions between the thiophene moieties in the acceptor groups of porphyrin and the protons of the acidic conditions tend to enhance the hydrogen evolution efficiency over PCT-LG-23 composite. The photoelectrochemical studies confirm the charge-transfer efficiency and the chemical reactivity of the composites indicating their efficacy and efficiency. To achieve better solar water splitting performance, further consideration of the molecular design of zinc porphyrin-based sensitizers is in progress.

Conflicts of interest

There are no conflicts to declare.

Acknowledgements

This work was supported by the DAE/BRNS No: 34/14/03/2018-BRNS/34079 and DST/TMD/HFC/2k18/60. N. C. and S. G. thanks to AcSIR for their PhD enrolment. DK and LG thank Newton-Bhabha prize grant for the financial support. We are thankful to Dr S. Chandrasekhar, Director, Dr N. V. Satyanarayana, and HOD in DEEE of CSIR-IICT for providing research facilities. CSIR-IICT Communication no: IICT/Pubs./2020/018.

References

1 A. Fujishima and K. Honda, Electrochemical Photolysis of Water at a Semiconductor Electrode, *Nature*, 1972, **238**, 37–38.
2 A. Naldoni, M. Altomare, G. Zoppellaro, N. Liu, S. Kment, R. Zboril and P. Schmuki, Photocatalysis with Reduced TiO_2: From Black TiO_2 to Co-catalyst-Free Hydrogen Production, *ACS Catal.*, 2019, **9**, 345–364.
3 A. Dutta, S. K. Dutta, S. K. Mehetor, I. Mondal, U. Pal and N. Pradhan, Oriented Attachments and Formation of Ring-on-Disk Heterostructure Au–Cu_3P Photocatalysts, *Chem. Mater.*, 2016, **28**, 1872–1878.

4 M. J. Torralvo, J. Sanz, I. Sobrados, J. Soria, C. Garlisi, G. Palmisano, S. Cetinkaya, S. Yurdakal and V. Augugliaro, Anatase photocatalyst with supported low crystalline TiO_2: The influence of amorphous phase on the activity, *Appl. Catal., B*, 2018, **221**, 140–151.

5 T. Song, P. Zhang, J. Zeng, T. Wang, A. Ali and H. Zeng, Boosting the photocatalytic H_2 evolution activity of Fe_2O_3 polymorphs (α-, γ-, and β-Fe_2O_3) by fullerene [C60]-modification and dye-sensitization under visible light irradiation, *RSC Adv.*, 2017, **7**, 29184–29192.

6 N. Kaeffer, C. D. Windle, R. Brisse, C. Gablin, D. Leonard, B. Jousselme, M. C. Kerlidou and V. Artero, Insights into the mechanism and aging of a noble- metal free H_2- evolving dye-sensitized photocathode, *Chem. Sci.*, 2018, **9**, 6721–6738.

7 J. Kim, D. R. Whang and S. Y. Park, Designing highly efficient Cu^I photosensitizers for photocatalytic H_2 evolution from water, *ChemSusChem*, 2017, **10**, 883–1886.

8 Y. Zheng, J. Wang, J. Zhang, T. Peng and R. Li, Syntheses of asymmetric zinc porphyrins bearing different pseudopyrdine substituents and their photosensitization for visible-light-driven H_2 production activity, *Dalton Trans.*, 2017, **46**, 8219–8228.

9 P. Y. Ho, M. F. Mark, Y. Wang, S. C. Yiu, W. H. Yu, C. L. Ho, D. W. McCamant, R. Eisenberg and S. Huang, Panchromatic sensitization with Zn^{II} Porphyrin-based photosensitizers for light-driven hydrogen production, *ChemSusChem*, 2018, **11**, 1–13.

10 E. Koposova, X. Liu, A. Pendin, B. Thiele, G. Shumilova, Y. Ermolenko, A. Offenhausser and Y. Mourzina, The influence of meso-substitution of the porphyrin ring on enhanced hydrogen evolution in a photochemical system, *J. Phys. Chem. C*, 2016, **120**, 13873–13890.

11 J. Wang, Y. Zheng, T. Peng, J. Zhang and R. Li, Asymmetric zinc porphyrin derivative-sensitized graphitic carbon nitride for efficient visible-light- driven H_2 production, *ACS Sustainable Chem. Eng.*, 2017, **5**, 7549–7556.

12 P. S. Gangadhar, S. Gonuguntla, S. Madanaboina, N. Islavath, U. Pal and G. Lingamallu, Unravelling the impact of thiophene auxiliary in new porphyrin sensitizers for high solar energy conversion, *J. Photochem. Photobiol., A*, 2020, **392**, 112408.

13 H. Song, Q. Liu and Y. Xie, Porphyrin-sensitized solar cells: systematic molecular optimization, coadsorption and cosensization, *Chem. Commun.*, 2018, **54**, 1811–1824.

14 X. Zhang, T. Peng and S. Song, Recent advances in dye-sensitized semiconductor systems for photocatalytic hydrogen production, *J. Mater. Chem. A*, 2016, **4**, 2365–2402.

15 P. Liao, Y. Hu, Z. Liang, J. Zhang, H. Yang, L. Q. He, Y. X. Tong, J. M. Liu, L. Chen and C. Y. Su, Porphyrin-based imine gels for enhanced visible-light photocatalytic hydrogen production, *J. Mater. Chem. A*, 2018, **6**, 3195–3201.

16 Z. Chen, J. Wang, S. Zhang, Y. Zhang, J. Zhang, R. Li and T. Peng, Porphyrin-Based Conjugated Polymers as Intrinsic Semiconducting Photocatalysts for Robust H_2 Generation under Visible Light, *ACS Appl. Energy Mater.*, 2019, **2**, 5665–5676.

17 L. Li, G. B. Bodedla, Z. Liu and X. Zhu, Naphthalimide-porphyrin hybridized graphitic carbon nitride for enhanced photocatalytic hydrogen production, *Appl. Surf. Sci.*, 2020, **499**, 143755.

18 L. Y. Huang, J. F. Huang, Y. Lei, S. Qin and J. M. Liu, Porous hybrid materials based in mesotetrakis(Hydroxyphenyl) Porphyrins and TiO_2 for efficient visible-light-driven hydrogen production, *Catalysts*, 2020, **10**, 656.

19 X. Guo, X. Li, L. Qin, S. Z. Kang and G. Li, A highly active nano-micro hybrid derived from Cu-bridged TiO_2/porphyrin for enhanced photocatalytic hydrogen production, *Appl. Catal., B*, 2020, **268**, 118434.

20 Z. Zhang and Y. Zhu, Xianjie Chen, Hanjie Zhang, and Jun Wang, A Full-Spectrum Metal-Free Porphyrin Supramolecular Photocatalyst for Dual Functions of Highly Efficient Hydrogen and Oxygen Evolution, *Adv. Mater.*, 2018, **31**, 1806626.

21 M. Xi, P. Wang, M. Zhang, L. Qin, S. Z. Kang and X. Li, ZnO nanorods/sulfophenyl porphyrin nanocomposites facilely embedded with special copper for improved photocatalytic hydrogen evolution, *Appl. Surf. Sci.*, 2020, **529**, 147200.

22 D. N. Tritton, G. B. Bodedla, G. Tang, J. Zhao, C. S. Kwan, K. C. F. Leung, W. Y. Wong and X. Zhu, Iridium motif linked porphyrins for efficient light-driven hydrogen evolution *via* triplet state stabilization of porphyrin, *J. Mater. Chem. A*, 2020, **8**, 3005–3010.

23 S. Gonuguntla, A. Tiwari, S. Madanaboina, L. Giribabu and U. Pal, Revealing high hydrogen evolution activity in zinc porphyrin sensitized hierarchical porous TiO_2 photocatalysts, *Int. J. Hydrogen Energy*, 2020, **45**, 7508–7516.

24 P. S. Gangadhar, S. Gonuguntla, S. Mandanaboina, N. Islavath, U. Pal and L. Giribabu, Unravelling the impact of thiophene auxillary in new porphyrin sensitizers for high solar energy conversion, *J. Photochem. Photobiol., A*, 2020, **392**, 112408.

25 N. V. Krishna, J. V. S. Krishna, S. P. Singh, L. Giribabu, L. Han, I. Bedja, R. K. Gupta and A. Islam, Donor-π-Acceptor based stable porphyrin sensitizers for dye-sensitized solar cells: effect of π-conjugated spacers, *J. Phys. Chem. C*, 2017, **121**, 6464–6477.

26 K. Devulapally, G. Reddy, S. Prasanthkumar, A. Jagadeesh, S. Soman and L. Giribabu, Effect of auxillary acceptor on D-π-A based porphyrin sensitizers for dye sensitized solar cells, *J. Porphyrins Phthalocyanines*, 2021, **25**, 407–417.

27 A. Tiwari, N. V. Krishna, L. Giribabu and U. Pal, Hierarchical Porous TiO_2 Embedded Unsymmetrical Zn-Phthalocyanine Sensitizer for Visible-Light-Induced Photocatalytic H_2 Production., *J. Phys. Chem. C*, 2018, **122**, 495–502.

28 L. Zhang, L. Han, P. Peng Hu, L. Wang and L. Dong, TiO_2 nanotube arrays:intrinsic peroxidase mimetics., *Chem. Commun.*, 2013, **49**, 10480–10482.

29 G. I. N. Waterhouse, A. K. Wahab, M. Al-Oufi, V. Jovic, D. H. Anjum, D. Sun-Waterhouse, J. Llorca and H. Idriss, Hydrogen production by Tuning the Photonic Band Gap with the Electronic Band Gap of TiO_2, *Sci. Rep.*, 2013, **3**, 2849.

30 M. J. Frisch, G. W. Trucks, H. B. Schlegel, G. E. Scuseria, M. A. Robb, J. R. Cheeseman, G. Scalmani, V. Barone, G. A. Petersson and H. Nakatsuji, *Gaussian 16, Revis. B.01*, 2016.
31 N. M. Oboyle, A. L. Tenderholt and K. M. Langner, *J. Comput. Chem.*, 2008, **29**, 839–845.
32 O. Suryani, Y. Higashino, H. Sato and Y. Kubo, Visible-to-Near-Infrared Light-Driven Photocatalytic Hydrogen Production Using Dibenzo-BODIPY and Phenothiazine Conjugate as Organic Photosensitizer, *ACS Appl. Energy Mater.*, 2019, **2**, 448–458.